Case Studies in Construction Materials 16 (2022) e00993

Contents lists available at ScienceDirect

Case Studies in Construction Materials

journal homepage: www.elsevier.com/locate/cscm

# Development of a multifunctional nanocomposite system for protection, consolidation and microbial growth prevention of porous stones: A case study for the conservation of tuff

Annalisa Apicella, Lucia D'Arienzo, Sara Caridi, Arianna Pietrosanto, Paola Scarfato *

*Department of Industrial Engineering, University of Salerno, Via Giovanni Paolo II, 132-84084 Fisciano, SA, Italy*

ARTICLE INFO

*Keywords:*
Nanocomposite
Tuff stone
Surface treatment
Water-repellency
Consolidant
Biocide

ABSTRACT

In this work, innovative, sustainable, multifunctional surface treatments for tuff protection that combine water-repellency, consolidating function and long-lasting antimicrobial activity were developed and tested. In particular, different water-based formulations were prepared by adding to a commercial polysiloxane treatment a biocide against biodeterioration, or clay nanoparticles to strengthen the tuff or their combination where the biocide was partially loaded into the nanoclay to join protective, consolidant and long-lasting biocide activity. The last formulation showed the best overall performances, since the constituents synergically improve its water-repellency and aggregative effectiveness without changing the color. Moreover, all surface treatments showed promising antimicrobial activity.

## 1. Introduction

Conservation of buildings and cultural heritages is one of the greatest challenges of contemporary research. Among the many natural building materials used all along history, tuff stone, an igneous rock of volcanic origin, is one of the most vulnerable, because of its porous nature, which promotes water penetration into its structure and microorganism growth on its surface. Tuff stones are used in many world countries and, where available, they were commonly used for construction. In Italy, for example, tuff stones are typical features of the Romans Republican and early Imperial buildings and monuments. In particular, this volcanic rock is widely spread in the Campania region (Southern Italy) and its excellent workability contributed to its great fortune in the historical building of this area [1–3]. Nevertheless, due to its macro-porous texture, mineralogical composition and high bioreceptivity, relevant degradation processes affect tuff stone [4–6]. Water has a key role in the deterioration mechanisms of the tuffs because it easily penetrates the material, which has a strong hydrophilic character and high capillary porosity, thus carrying corrosive or reactant substances, dissolving soluble constituents, inducing high tensile stresses if freezed and promoting microbial activity [7–9]. Therefore, reducing the tuff hydrophilicity is an essential tool to counteract the chemical-physical and biological phenomena that cause its deterioration.

To obtain this goal, many water-repellent polymer protection systems were developed, mostly based on silicone, siloxane and acrylic resins and fluorinated polymers [10–14]. All of them are effective hydrophobizing agents since they strongly reduce the water

* Corresponding author.
*E-mail addresses:* anapicella@unisa.it (A. Apicella), ldarienzo@unisa.it (L. D'Arienzo), ing.caridi@gmail.com (S. Caridi), arpietrosanto@unisa.it (A. Pietrosanto), pscarfato@unisa.it (P. Scarfato).

https://doi.org/10.1016/j.cscm.2022.e00993
Received 29 October 2021; Received in revised form 21 February 2022; Accepted 2 March 2022
Available online 4 March 2022
2214-5095/© 2022 The Authors. Published by Elsevier Ltd. This is an open access article under the CC BY license (http://creativecommons.org/licenses/by/4.0/).

permeability of the substrates, but often show limited performances in restoration processes, where additional requirements should be satisfied, such as e.g., surface consolidation, transparency, photo-oxidative stability, compatibility with the substrate, etc., or against other degradation factors as the microbial growth. Thus, to inhibit the proliferation of microorganisms the most widespread and easy way is the additional use of biocides, which however have often short durability, because of their leaching and denaturation phenomena [15–20]. Hence, new high performing, multifunctional and durable treatments are still required.

The last few years have seen the rising of many studies on nanotechnologies in the preservation and restoration of building materials and cultural heritages, as they could overcome some limits of conventional protective methods [21–39]. Manoudis et al. were among the first (2007) to test nanocomposite polymer-silica films as protective coatings for stone-based monuments [21]. Other authors tested different nanosilica-based formulations on several substrates (tuff, marble, sandstones, limestone, etc.) to develop smart surfaces capable of preventing deterioration processes from starting [22–27]. D'Arienzo et al. proposed a nanocomposite treatment based on an organomodified nanoclay and a fluoroelastomer-acrylic resin for protection and consolidation of Neapolitan yellow tuff [28]. Cappelletti et al. tested the addition of $TiO_2$ nanoparticles to a commercial water-repellent for protection of several stone substrates (Botticino marble, Carrara marble and Angera stone), getting superhydrophobic surfaces, with no aesthetical alteration [29]. More recently, Chatzigrigoriou et al. (2020) obtained superhydrophobicity using siloxane resin and $Ca(OH)_2$ nanoparticles for marble protection [30]. D'Orazio and Grippo, instead, used $TiO_2$ nanoparticles in poly(carbonate urethane) formulations to treat tuff surfaces [31]. Then, Lettieri et al. exploited nanostructured $TiO_2$ stone coatings analyzing their compatibility with the substrate and the self-cleaning behavior [32]. Recently, nanocomposite treatments incorporating biocide activity were developed by Ditaranto et al. and Van Der Werf et al., which used Cu and Zn nanoparticles embedded in a polysiloxanic matrix as novel conservation treatments [35, 36], by Scarfato et al. (2016), which developed and evaluated halloysite nanotube-based biocide carrier for construction materials protection [37] and also by Zarzuela et al. (2018), which evaluate the effectiveness of a nano-structured multifunctional treatment, that combine consolidant and biocidal action, on different stones [38].

In this work, we report the results of a preliminary experimental study on an innovative, multifunctional surface treatment for tuff protection, able to ensure at the same time water-repellency, consolidating function and long-lasting antimicrobial activity, in a water-based environmentally friendly, nontoxic formulation. For this purpose, a commercial protective/consolidant oligosiloxanic resin was used as the base for designing new treatment systems incorporating alternatively a wide range biocide, a natural layered nanoclay (sodium montmorillonite) and their combination. In the latter case, however, part of the biocide was intercalated into the interlayer space of nanoclay, which therefore acts as carrier and offers a potential for a delayed release of the biocide. The effectiveness of the multifunctional surface treatments was evaluated by applying them on tuff substrates that were then submitted to water capillary absorption tests, static contact angle measurement, abrasion tests, colorimetric analysis and preliminary microbiological tests.

## 2. Experimental section

### 2.1. Materials

The protective treatment used for the experiments was the Silo 112 (hereinafter referred to as OS), a water-repellent formulation commonly used to treat historical and artistic surfaces, produced and commercialized by CTS s.r.l. (Altavilla Vicentina – VI, Italy). It is a mixture of organosiloxane oligomers dispersed in demineralized water and it is completely solvent free. Its reactive organosiloxane oligomers, consisting of a few tens of monomers, can deeply penetrate stone pores before they crosslink, usually after 24–48 h since their application. They impart excellent waterproofness to the treated surfaces without forming any superficial film impervious to water vapor, thus maintaining high vapor permeability of the tuff substrate [40]. OS is particularly recommended to treat limestones and silicate stones, as well as for paintings and fine plasters, because it does not change the exterior aspect of the surface. The specific properties of the product, as reported in the technical sheet, and the dry matter measured after curing for 24 h at room temperature, are denoted in Table 1.

Biotin T (hereinafter referred to as B) is a commercial biocide with a wide range, active against lichenes, fungi and algae, produced and commercialized by CTS s.r.l. (Altavilla Vicentina – VI, Italy). It's a water based liquid composition containing as active principles alkyl-benzyl-dimethyl-ammonium chloride (referred as quaternary ammonium salt), formic acid and n-octyl-isothiazolinone (OIT). The specific properties of the product, as reported in the technical sheet, are listed in Table 2.

Commercial sodium montmorillonite with trade name of Cloisite Na+ (referred as CNa; cation exchange capacity: 92.6 meq/100 g; d001 basal spacing: 11.7 Å) was purchased from Southern Clay Products Inc. (USA), having molecular formula $[Na_{0.75}(Al_{3.25}Mg_{0.75})(Si_8O_{20})(OH)_4]$. Montmorillonite clay particles are characterized by stacks of aluminosilicate layers (of about 1 nm thick) with gaps in

**Table 1**
Main properties of the OS product used as protective surface treatment.

| *Description* | Water-based, water repellent protective for construction materials of historic interest |
|---|---|
| *Active material* | Organosiloxane oligomers |
| *Active material content (%)* | 10 |
| *Solvent* | Demineralized water |
| *Appearance* | Milky liquid |
| *pH* | 7–8 |
| *Density at 20 °C (g/ml)* | 1.0 |
| *Dry matter after 24 h curing (%)* | 7 |

**Table 2**
Main properties of the biocide formulation.

| *Description* | Concentrate preservative for building materials Water dilutable |
|---|---|
| *Active principle* | n-octyl- isothiazolinone and quaternary ammonium salts |
| *Solvent* | Demineralized water |
| *Appearance* | Colorless to yellow liquid |
| *pH* | 5.5 (2% solution) |
| *Density at 20 °C (g/ml)* | 0.94 |
| *Stability* | Temperature from − 5 °C to + 80 °C |

between them. The lateral dimensions of the layered sheets are 0.1 μm to more than 1 μm [41].

Not-weathered Neapolitan yellow tuff stones (density 1.10 g/cm$^3$, collected in a quarry located in Comiziano, Naples, Italy), cut into cubic specimens (side length 5 cm), have been used as a substrate. Fig. 1 reports its x-ray diffractogram (a) and a SEM image (b). XRD spectrum shows the presence of the main mineralogical components: phillipsite (Phi), chabazite (Cha), segelerite (Se) and analcime (An) [11,42]. Accordingly, the SEM micrograph shows rod-shaped phillipsite and pseudo-cubic chabasite crystals aggregated in crusts and granular masses.

### 2.2. Preparation of samples

CNa clay was loaded with the biocide according to the following procedure: (1) sonication of 5.0 g of clay powder in 20 ml of B (for 30 min at room temperature), to increase the clay layer interspace; (2) magnetic stirring (24 h, 50 °C); (3) recovery of the solid matter by centrifugation; (4) washing (for removal of the unloaded biocide, by suspension in water/acetone (1:1 by volume)) and centrifugation, and air drying. The amount of biocide loaded into the clay was equal to 24.3 wt%, as determined by thermogravimetric analysis (see the Result and discussion section). In the following, the loaded clay system will be referred to as CNaB.

After, by using B, CNa and CNaB as co-formulating agents, three different surface treatments based on OS were prepared by mechanical stirring. according to the compositions and nomenclature reported in Table 3, together with the corresponding pH and viscosity values.

In all systems, the loading amounts of the constituents were selected in order to give a final B content of ca. 2%, as recommended by the producer, and a clay content of ca. 3 wt%, chosen on the basis of our previous studies on other nanocomposite systems for tuff protection [28,33,37]. The OS_CNaB system formulation was set in order to combine the same B and CNa content of the OS_B and the OS_CNa ones, respectively. For this, part of B was added as liquid formulation, and therefore is immediately available for antimicrobial action, and part was added as B loaded into the clay (i.e. CNaB), thus it must be released from the clay before being able to act, which could prolong the activity of the system over time.

Then, the prepared systems were applied on the specimens in two layers by paint-brushing, according to the producer recommendations (yield ~ 4 g/dm$^2$). All treated samples were left to age for 24 h at room conditions before being analyzed, to ensure that the crosslinking reaction of the organosiloxane oligomers was completed.

### 2.3. Characterization methods

X-ray diffraction (XRD) analyses were performed with a Bruker D8 Advance diffractometer (Ni-filtered CuKα radiation λ = 1.5418 Å, 40 kV, 40 mA). Diffraction patterns were recorded in the 2θ angular range of 5–70° at a scanning rate of 0.5 deg/min.

Scanning electron microscopy (SEM) analysis was carried out with a LEO 420 apparatus (LEO Electron Microscopy Ltd.) operated at

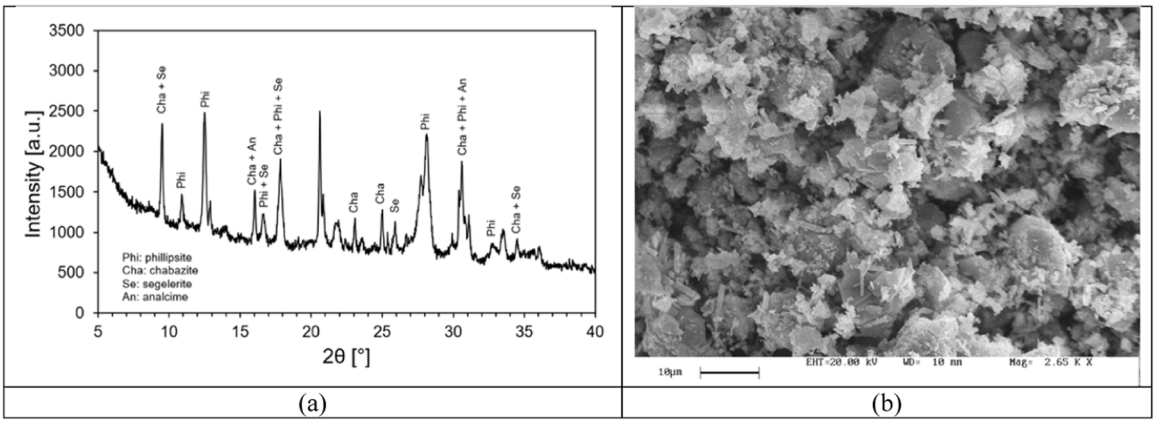


**Fig. 1.** XRD pattern and SEM image of the tuff stone used as substrate.

**Table 3**
Nomenclature and composition of the prepared treatments.

| | Sample composition [%] | | | | pH | Viscosity [mPa·s] |
|---|---|---|---|---|---|---|
| Sample name | OS | B | CNa | CNaB | | |
| *OS* | 100 | – | – | | 7.0 | 17.0 ± 1.8 |
| *OS_B* | 98 | 2 | – | | 6.7 | 16.5 ± 1.6 |
| *OS_CNa* | 97 | – | 3 | | 7.9 | 23.5 ± 2.9 |
| *OS_CNaB* | 95 | 1 | | 4[a] | 7.3 | 20.1 ± 2.1 |

[a] consisting - as determined by TGA analysis - of 0.97% of B loaded into the clay and 3.03% of CNa, thus getting a formulation containing a total amount of B and CNa equal to ~2.0% and ~ 3.0%, respectively.

20 kV. The images were taken on AuPd sputter-coated fractured tuff sections.

The pH was measured in triplicate using MACHEREY-NAGEL pH-indicator test strips (pH-Fix 6.0–10.0).

Viscosity measurements were performed using a rotational viscometer HAAKE Viscotester C (Thermo Scientific, USA) at 20 °C and 200 rpm, using the L1 spindle.

Thermogravimetric analyses (TGA) were performed using a SHIMADZU TGA-50WSI analyzer. Analyses were performed over the temperature range 30÷900 °C operating at a high resolution heating ramp of 10 °C/min (resolution 3.0 °C) in a nitrogen atmosphere. The tests were performed in triplicate.

Fourier Transform Infrared (FT-IR) spectra were obtained using a Thermo Nicolet Nexus spectrometer (Thermo Scientific, USA), equipped with a Globar IR source and a potassium bromide (KBr) beam splitter. The measurements were performed in transmission mode on powder samples, prepared by grinding them with KBr powder (FT-IR grade) and pressing the ground mixture into a disk. The samples were scanned 64 times with a resolution of 2 $cm^{-1}$ over the wavenumbers range from 4000 to 500 $cm^{-1}$. The spectral analyses were performed using an Omnic spectra analyzer.

The penetration depth of the protective treatments inside the tuff was evaluated was measured on fracture surfaces of paint-brushed specimens. After complete crosslinking of the treatment, the fracture surfaces of the samples were wetted with water and observed. For a clearer view, the measures were also made on tuff specimens paint brushed with solutions of the treatments added with a red water-soluble dye.

Static contact angle measurements were performed with a First Ten Angstrom Analyzer System 32.0 (mod. FTA 1000). The tests were carried out on clay powder samples pressed into a disk, using distilled water as test liquid. The reported results are the average of five replicate measurements on each sample. Static contact angle measurements were also performed on tuff samples both untreated and treated with the protective systems.

Capillary water absorption tests were performed according to the European Standard UNI EN 15801 (2010) [43] on cubic tuff specimens (5x5x5 $cm^3$), both untreated and treated on one face by paint-brushing with the different protective systems. The specimens were immersed in water at a depth of 3–4 mm (kept constant for the duration of the experiment) and the weight increase resulting from the absorption of water by capillarity was measured as a function of the time. The capillary water uptake typically fits the following equations [44]:

$$\Delta W = [(m_i - m_o)/A] \quad (1)$$

$$\Delta W = WAC \cdot t^{1/2} \quad (2)$$

In Eq. (1) ΔW is the mass increase (g) of absorbed water by the exposed area A ($cm^2$). WAC ($g \cdot cm^2 \cdot s^{-1/2}$) represents the water absorption coefficient and it can be calculated by the Eq. (2) as the slope of the linear section in the first step of the capillary absorption test. The tests were performed on five replicate specimens, obtaining a relative standard deviation always lower than 8%.

The abrasion resistance of both treated and untreated stones was carried out by means of the Taber Linear Abrasion Tester (Model 5700) equipped with P120 grade abrasive discs. Each sample was abraded under a weight of 750 g, by performing 150 runs at 40 runs/min. The aggregative efficacy [45] was determined according to the formula:

$$AE\ \% = 100 \times (\Delta M_{untr} - \Delta M_{tr}) / \Delta M_{untr} \quad (3)$$

where $\Delta M_{untr}$ is the average difference in the untreated samples between the weight values before and after 150 abrasive runs; $\Delta M_{tr}$ is the difference between the initial weight and the weight after 150 abrasive runs measured for each treated sample. The tests were performed in triplicate, obtaining a relative standard deviation always lower than 5%.

Colorimetric analysis was carried out on the untreated and treated tuff samples with a CR-410 HEAD colorimeter (Konica Minolta Sensing, Inc.), based on the L*, a* and b* coordinates of the CIELAB space, according to the Italian Recommendation NORMAL 43/93 [46]. Namely, the L* values range from 0 to + 100 and represent black and white, respectively, the negative and positive a* values represent green and red, respectively, while the negative and positive b* values represent blue and yellow. From the parameters above, the total color difference, ΔE, is calculated using the untreated tuff sample as a reference, according to the formula: $\Delta E = (\Delta L^{*2} + \Delta a^{*2} + \Delta b^{*2})^{1/2}$. The reported ΔE values are the mean value of five measures per area.

### 2.4. Preliminary microbiological tests

To verify the efficacy of the biocide against microbial proliferation, preliminary in vitro microbiological tests were carried out against a mold sample previously collected by scraping the walls of an encrusted tuff substratum with a sterile scalpel [47].

The material was deposited onto a sterile Petri dish containing YEPD-agar (Yeast Extract Peptone Dextrose Agar), a non-selective solid medium for the growth of yeasts and molds, prepared according to the composition of the following Table 4.

Subcultures were grown aerobically overnight at 37 °C in an incubator. In order to collect the spores to be inoculated, 500 μL of physiological saline mixed with 0.05% v/v Tween 80 surfactant were gently poured onto the Petri dish and then recovered. The sample was serially diluted in 10-fold steps to 10–8 and aliquots containing 10 μL of each dilution were spread onto the antimicrobial-loaded plates prepared as follows (20 ml per each): (a) YEPD-agar (negative control); (b) YEPD-agar + 1% B; (c) YEPD-agar + 2% B; (d) YEPD-agar + 1.08% B + 3% CNaB (corresponding to a total amount of B equal to 2%).

The inoculated plates were left in the incubator for 48 h at 37 °C, to promote the growth of microorganisms. At the end of the incubation, the plates were examined for microbial growth. Counts were performed in triplicate.

## 3. Results and discussion

### 3.1. Characterization of biocide-loaded nanoclay

Thermogravimetric analysis has been carried out for both neat and loaded nanoclay, in order to quantify the amount of biocide incorporated into the mineral. The results are compared in Fig. 2.

The neat CNa shows three weight loss steps: the first one, in the 30–100 °C range, is attributed to the free water volatilization; the next one, in the 200–550 °C range, is rather small and can be associated to dehydroxylation of kaolinite group minerals contained as impurities in the CNa; the last one, at T > 550 °C, is due to the structural water loss resulting from montmorillonite clay dehydroxylation [41].

The CNaB sample also has the first weight loss below 100 °C, which can be ascribed to free water and biocide volatile constituents' removal. However, with respect to the neat CNa, the CNaB clay shows a lower weight loss in this T range, which indicates that the loaded clay contains less free water. This suggests that the clay acquires a more hydrophobic character after the loading of the biocide components, which can both enter the clay galleries and be adsorbed on clay surfaces, occupying hydrophilic binding sites that are consequently unable to form hydrogen bonds with the water. A higher temperature, in the 200–550 °C range, the CNaB curve shows a second two-stage decomposition zone, corresponding to the organic compounds' degradation processes. The last decomposition zone, at T > 550 °C, is ascribed to dehydroxylation of both montmorillonite clay and oligosiloxanic constituents of biocide. The amount of biocide loaded in CNaB was 24.3 ± 1.2 wt%, as calculated from the difference between the weight change % in the range 120–900 °C of the loaded CNaB (68.5 wt%) and the neat CNa (92.8 wt%).

With the aim to verify if the biocide has been simply adsorbed on the clay surface, only modifying the powder wettability, or has also entered the clay galleries so increasing the basal interlayer distance, too, static contact angle and X-ray diffraction experiments were carried out on pristine and loaded clays.

Static contact angle experiments were carried out on powder samples of neat CNa and CNaB pressed into disks, using distilled water as test liquid. The images of the sessile drops deposited on the two disks and the corresponding contact angle (CA) values are reported in Fig. 3. The photos clearly show that the water wettability of the neat clay is significantly reduced after its treatment with the antimicrobial agent since the CA increases from 44° for CNa up to 68.9° for CNaB. The phenomenon can be explained considering that the biocide constituents were adsorbed on the clay surface: here they act as surfactants therefore they lower the clay surface energy and convert the surface hydrophilic character of CNa into a more organophilic one [48]. A further contribution to the observed wettability change can also be given by the occlusion of the clay galleries due to the biocide entry.

The XRD spectra are reported in Fig. 4. The patterns clearly evidence the shift of the characteristic peak of the unloaded sample CNa from its original position (2θ = 7.2°) to lower diffraction angles (2θ = 5.0°) in the CNaB loaded system. This shift indicates an enlargement in the clay mineral interlayers with the basal d-spacing passing from 1.17 nm to 1.76 nm, so confirming that the biocide, in addition to being adsorbed on the clay surface, also penetrated the clay galleries.

To ensure that the performed loading process has not chemically altered the biocide, FT-IR analysis was carried out on the neat and loaded clay and on the biocide. The corresponding spectra are compared in Fig. 5. The CNa trace shows the following absorption bands: at 3633 $cm^{-1}$ the O-H stretching vibration of Al–OH and Si–OH; at 3440 $cm^{-1}$ related the broad –OH stretching of the interlayer water; at 1637 $cm^{-1}$ and 1044 $cm^{-1}$ the interlayer water deformation vibrations and the stretching of Si–O group, respectively [49,50]. The biocide spectrum shows: in the ca. 3600–3000 $cm^{-1}$ range the broad band due to N-H stretching of ammonium group; in the

**Table 4**
Composition of prepared culture medium.

| | YEPD-agar [g/L] |
|---|---|
| *Bacteriological peptone* | 20 |
| *Yeast Extract* | 10 |
| *Glucose* | 20 |
| *Agar* | 35 |

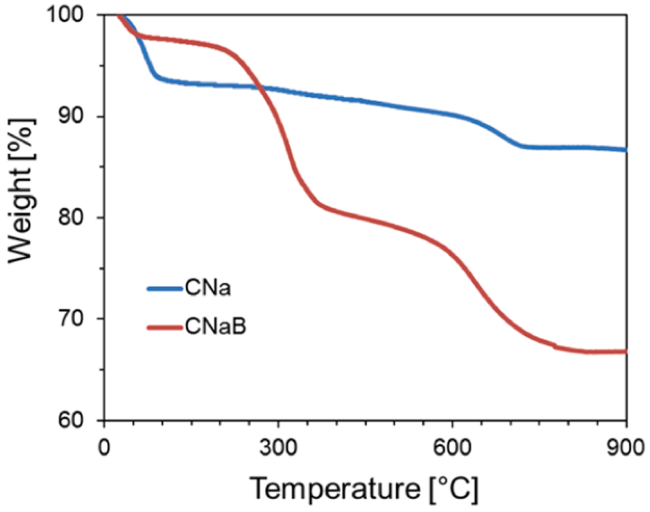


**Fig. 2.** TGA curves of neat CNa and CNaB.

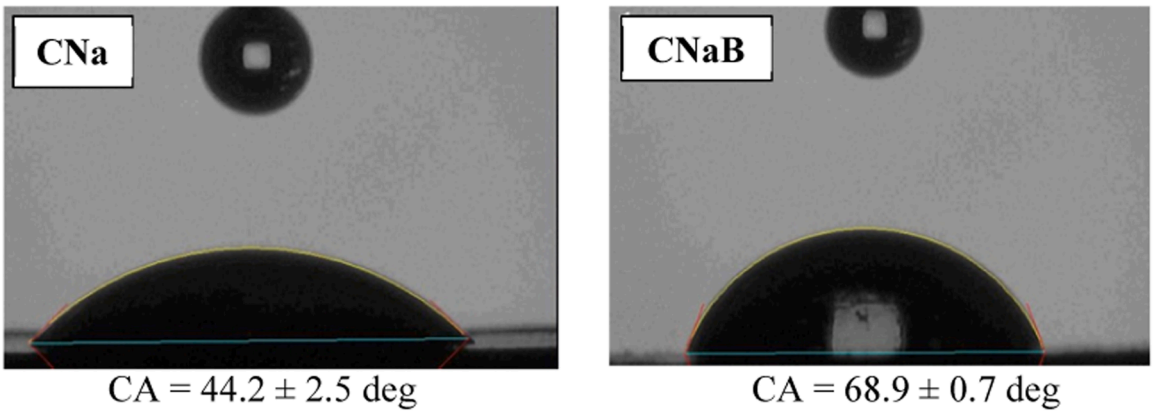


**Fig. 3.** Static contact angles (CA) of powder samples of neat CNa and CNaB pressed into disks.

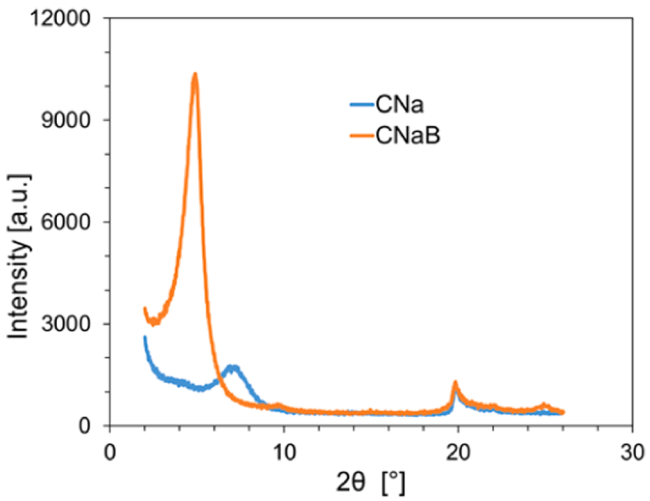


**Fig. 4.** XRD patterns for neat CNa and CNaB.

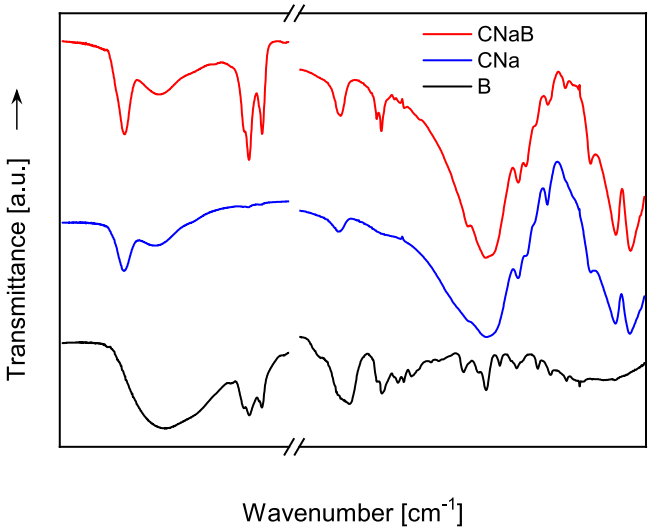


**Fig. 5.** FT-IR spectra of biocide, Cloisite $Na^+$ and loaded clay.

2800–2900 $cm^{-1}$ range the C-H stretching vibrations of the alkyls chains of the biocide quaternary ammonium salt; and at ca. 1600 $cm^{-1}$ the C = O stretching of the biocide isothiazolinone.

All the diagnostic signals of both neat CNa and biocide can be recognized, with no significant shift, in FT-IR spectrum of CNaB. This evidence demonstrates that the bioactive agent is loaded successfully into the natural clay, suggesting also that it has kept its chemical integrity, and thus its activity.

### 3.2. *Characterization of treated and untreated tuff samples*

The penetration depth of the treatments was evaluated on tuff samples paint brushed with the OS-based formulations. For a clearer view, the observation was also made using formulations added with a red water-soluble dye. As an example, Fig. 6 shows the pictures of the sections of tuff samples treated with OS. A depth of penetration of about 2.5÷3 mm was observed in the stones, independently on the applied treatment, as expected based on the small differences in terms of composition and viscosity of their formulations.

To investigate the waterproofing effectiveness of the developed biocide treatments on the tuff protection, tuff specimens, untreated and treated with the different protective systems, were submitted to static contact angle measurements and water capillary absorption tests. Table 5 reports the static contact angle values taken on all the samples.

As it can be seen from the table, the OS based treatments drastically change the hydrophilic character of the tuff stone. In fact, whereas it was not possible to record the static contact angle on untreated specimens due to the immediate absorption of test drops, all treated specimens show a clear hydrophobic behavior, with contact angle values well above 90°. In particular, the CA is approx. 125° for both the OS alone and its mixtures with the hydrophobic biocide and CNaB, whereas is 108.5° for the OS added with the hydrophilic CNa. At the same time, the treatments strongly affect the water absorption behavior too, as it comes out from Fig. 7, where it is reported the amount of absorbed water per unit of inflow surface, recorded versus time until 24 h.

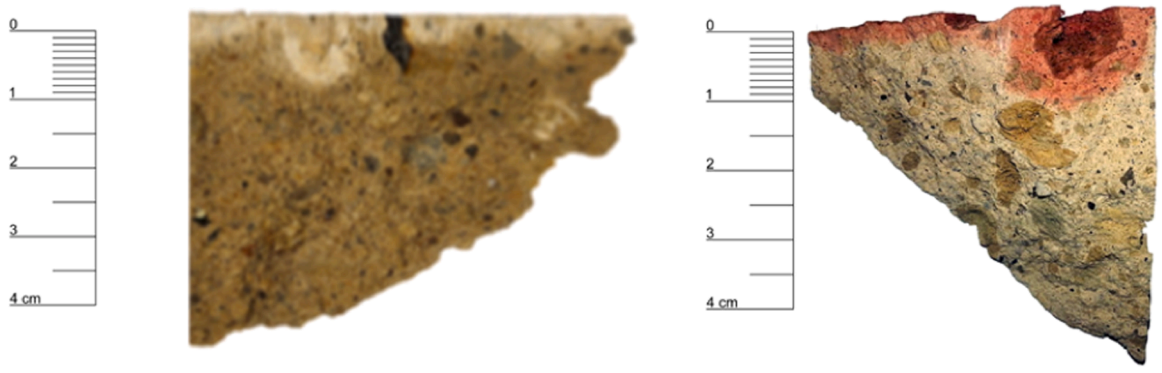


**Fig. 6.** Sections of tuff treated with OS, neat (left) or added with red water-soluble dye (right), for the estimation of the penetration depth of the treatments.

**Table 5**
Static contact angle (CA) values of treated and untreated tuff samples.

| SAMPLE | CA [deg] |
|---|---|
| *Untreated tuff* | not measurable |
| *OS* | 124.7 ± 1.6 |
| *OS_B* | 125.8 ± 1.3 |
| *OS_CNa* | 108.5 ± 1.0 |
| *OS_CNaB* | 127.5 ± 1.6 |

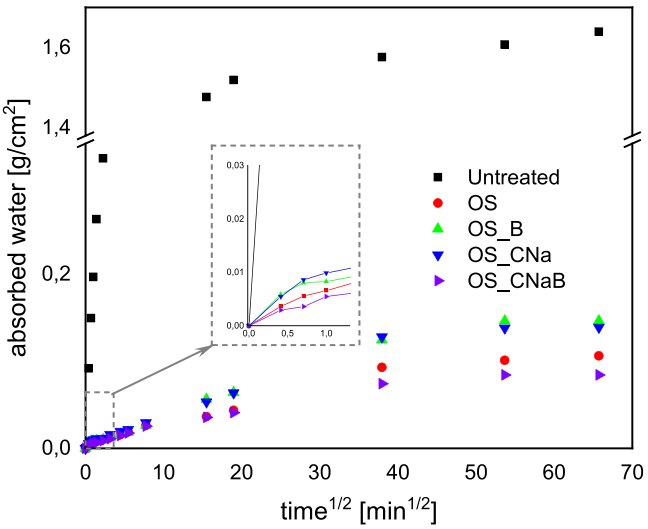


**Fig. 7.** Capillary absorption curves for treated and untreated tuff samples.

The graph shows that all the considered protective treatments markedly change the water capillary absorption behavior of the tuff. In fact, the untreated stone, due to its high open porosity and hydrophilic character, has a very fast water intake at short times, then reaching almost a plateau after ca. 4 h, when the specimen was saturated. On the other hand, all the treated stones have a very slower water absorption rate at short times, as it can be inferred from the lower initial slope of the curves. In fact, the corresponding values of the water capillary absorption coefficient, WAC, reported in Table 6, are about two orders of magnitude smaller than that of the untreated tuff.

Comparing the data, it clearly comes out that the most effective system in reducing both the tuff surface wettability and WAC was the OS_CNaB system, followed by OS and finally by OS_B and OS_CNa ones (the latter two roughly equivalent).

The hydrophilic/hydrophobic character of the treatment' constituents and the occurrence of synergic interaction between the biocide and the nanoclay can explain this trend. In particular, with respect to the original tuff, the application of the OS alone changes the tuff surface polar character - from hydrophilic to hydrophobic one – through the crosslinking of its organosiloxane oligomer constituents, as discussed above. The incorporation into the OS of the solely CNa nanoclay slightly reduces the OS' hydrophobic performance, which is coherent with the strong hydrophilic nature of the nanoclay [25,38]. Similar effect arises upon the addition of solely biocide: the biocide, although its hydrophobic character, can establish van der Waals and electrostatic interactions with the silanol groups of the oligosiloxane constituents, thus interfering with the crosslinking reaction and negatively influencing the OS effectiveness, once again to a limited extent [51,52]. On the contrary, significant benefits in terms of water repellence behavior, both at short and long-term, arise from the combined incorporation of CNa and B. The result can be explained as consequence of several synergic factors: (i) firstly, the B, which is both entrapped into the clay galleries and adsorbed on the clay surface, changes the nature of CNa from hydrophilic to hydrophobic: the modification of the surface character of the nanofiller reduces not only its swelling potential, but also its tendency to aggregate, thus leading to a better dispersion and distribution of the B-loaded clay a on a nano-scale into the liquid formulation [42,52]; (ii) secondly, the entrapment/adsorption of the biocide within the nanoclay prevents it from interacting with the crosslinking reaction of the organosiloxane oligomers. A similar synergic interaction between B and another natural nanoclay was also found in our previous published research [37], where a halloysite nanotube-based carrier for biocide activity in construction materials protection was developed and its effects on a mortar substrate wettability were investigated. Additional effects, arising from surface morphology changes after the application of the treatments, are expected to be poorly significant, similarly to what was found in another our study on yellow tuff treated with several nanoclay-based polymer protectives, where SEM observations revealed that the resin, both plain and nanocomposite, soaks the stone surface without significantly modify its morphology [28].

With the aim to evaluate possible consolidating effects of the OS based treatments, untreated and treated tuff samples were

**Table 6**
Water capillary absorption coefficient, WAC, and capillary water uptake at equilibrium for treated and untreated tuff samples.

| Sample | WAC·10$^3$ [g cm$^{-2}$ min$^{-1/2}$] | Capillary water uptake [g cm$^{-2}$] |
|---|---|---|
| *Untreated tuff* | 194 ± 14 | 1.640 ± 0.120 |
| *OS* | 6.51 ± 0.13 | 0.106 ± 0.011 |
| *OS_B* | 8.23 ± 0.16 | 0.146 ± 0.012 |
| *OS_CNa* | 9.21 ± 0.14 | 0.139 ± 0.012 |
| *OS_CNaB* | 4.92 ± 0.12 | 0.084 ± 0.008 |

submitted to abrasion tests according to the procedure reported in the Experimental section. The obtained results are reported in Table 7 in terms of Aggregative Efficacy, AE (i.e., difference of mass loss by abrasion among untreated and treated tuff, with respect to the untreated tuff, taken as a reference). The application of OS and OS_B treatments significantly increases the resistance to abrasion of the tuff with respect to the untreated one, giving aggregative efficacies of 30–31%. The benefits are even greater when the CNa and CNaB nanoclays are incorporated into the formulation, bringing the aggregative efficacies up to 41–45%. The strengthening comes from the ability of the OS siloxane oligomers to bond to silicates of the tuff surface creating strong crosslinked Si-O-Si bonding, which increases the grain-to-grain cohesion [53,54]. Additionally, in the case of the OS_CNa and OS_CNaB treatments, the nanoclays deposited into the pore structure of the tuff further improve the consolidating effect by reducing the pore size and participating in Si-O-Si chemical bonding. The slightly better performance of the OS_CNaB than the OS_CNa can be related to a greater number of dispersed nanoclay platelets into the first systems: the loading of biocide, in fact, make easier the clay swelling and reduces its tendency to staking, thus resulting in a higher exfoliation degree. In all cases, the reaction leaves the apolar groups of the organosiloxane protruding from the tuff surface, making it hydrophobic, too, as discussed above. Both the hydrophobization and the consolidation actions have a key role in improving the durability of treated tuff.

The aesthetic alteration of treated tuff surfaces was investigated by means of colorimetric measurements, collected after 48 h and 7 days since the application of the treatment. The results, in terms of chromatic change ΔE, are reported in Table 8.

The application of the OS treatments in all cases determine a variation in the color of the tuff substrate at short time (after 48 h), with ΔE values included in the 3.43–6.15 range. These values slightly decrease during time as the polymerization reactions evolves and the solvent (water) volatilizes; then, after 7 days, even in the worst case they are acceptable for stones subjected to consolidating and protective treatments, as also reported by other authors [22,55]. In particular, the OS_CNaB treatment gives the smallest chromatic change ($\Delta E < 3$) that, after 7 days since the application, can hardly be noticed and is almost negligible. The low color alteration measured for the tuff treated with OS_CNaB may arise from the high dispersion level of the nanoclay in this system and a high color similarity between the nanoclay and the tuff substrate used for the study ($\Delta E_{CNa/tuff} = 3.07 \pm 0.05$). Deeper analyses are needed to better clarify this point.

The effectiveness of the biocide percentage used to treat the tuff was verified with preliminary microbiological tests carried out against mold samples collected on encrusted tuff stone, according to the solid medium method described in the experimental section. Among the types of stone substrata, tuff, due to its high porosity values and surface roughness, is highly susceptible to colonization by several kinds of autotrophic microorganisms, including lichens, mosses, cyanobacteria and algae, and heterotrophic microorganism as fungi, which have been isolated from stone monuments located in different countries and cause bio-deterioration because of their complex metabolic activities on stone surface [56,57]. Fig. 8 shows the pictures of the tested plates after 48 h inoculated mold incubation at 37 °C. Five different systems were considered: (a) YEPD-agar (control); (b) YEPD-agar + 1% B; (c) YEPD-agar + 2% B; (d) YEPD-agar + 4% CNaB; and (e) YEPD-agar + 1% B + 4% CNaB, in order to discern the possible effects of both B concentration (1% as in (b) and (d), 2% as in (c) and (e)) and immobilization state (1% free as in (b) or entrapped into the clay as in (d)). After 48 h since the inoculation, the control plates exhibited a significant growth of the grafted fungi (Fig. 8(a)). In the presence of biocide concentration equal or higher than 1% (Fig. 8(b), (c), (d) and (e)), conversely, no viable cells could be detected, regardless of its immobilization state. These results indicate that all the developed biocide formulations are able to deliver the biocide sufficiently to inhibit the biological growth on the culture substrate, achieving an antimicrobial effect in vitro comparable with or higher than different micro- and/or nanoparticulated release systems containing bioactive agents widely used for building material protection and reported in literature [58,59]. Further studies are underway to examine the effectiveness of these systems over time, as a function of different substrates and of the different formulations developed.

**Table 7**
Aggregative Efficacy (AE) of treated tuff samples.

| Sample | AE [%] |
|---|---|
| *OS* | 30 ± 1 |
| *OS_B* | 31 ± 2 |
| *OS_CNa* | 41 ± 1 |
| *OS_CNaB* | 45 ± 2 |

**Table 8**
Color alteration of tuff specimens after the treatments.

| Sample | ΔE (after 48 h) | ΔE (after 7 days) |
|---|---|---|
| *OS* | 6.15 ± 0.04 | 5.12 ± 0.03 |
| *OS_B* | 5.15 ± 0.02 | 4.80 ± 0.04 |
| *OS_CNa* | 4.91 ± 0.04 | 4.85 ± 0.05 |
| *OS_CNaB* | 3.43 ± 0.02 | 2.58 ± 0.03 |

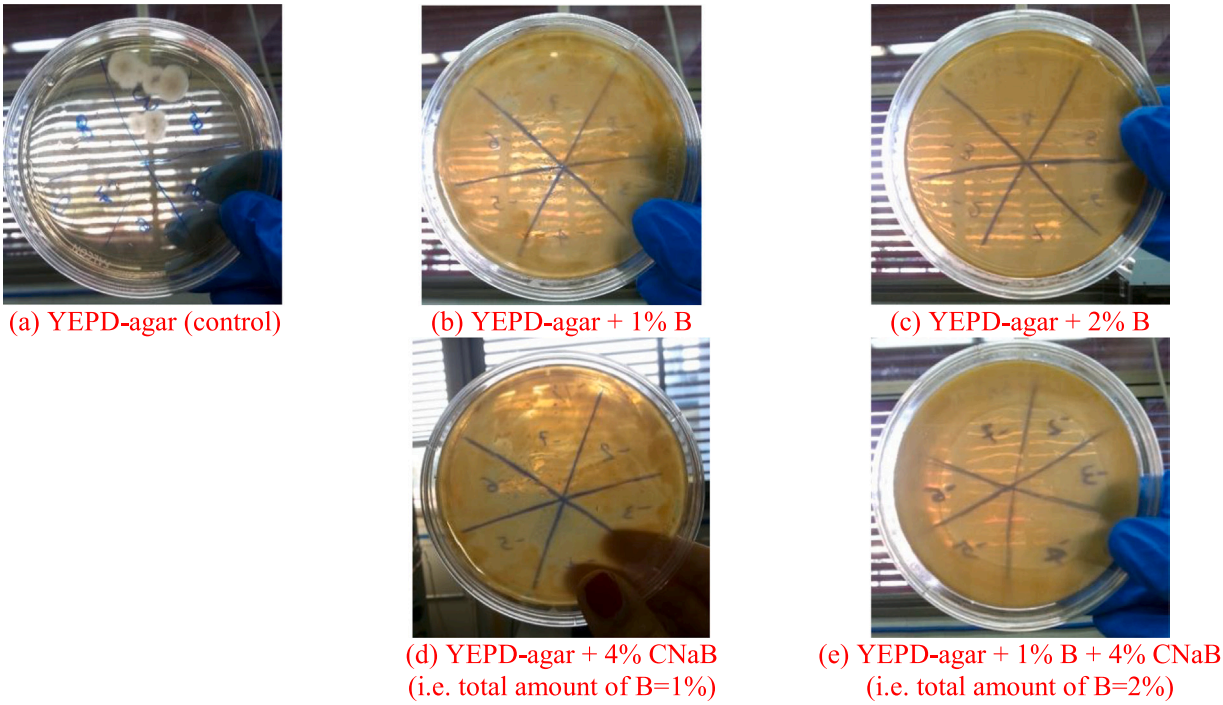


**Fig. 8.** Inoculated plates after 48 h.

## 4. Conclusions

In this work innovative and multifunctional surface treatments for hydrophobization, consolidation and protection from biodeterioration of tuff stone were developed and evaluated.

The treatments were prepared mixing a commercial water-repellent product with a nanoclay and/or a wide range biocide, added both as liquid formulation and loaded in the nanoclay.

All systems were demonstrated effective in modifying the tuff surface polar character from strongly hydrophilic to definitely hydrophobic one, with CA values in the range 108.5°– 127.5°. This has also brought benefits in terms of water capillary rise, for both absorption kinetic and amount of water absorbed at free saturation. The best performances were shown by the OS_CNaB. Its greater effectiveness was related to a synergistic action of its constituents that leads to the following benefits: the nanoclay loading with the biocide changes the CNa character from hydrophilic to hydrophobic, promotes higher dispersion level on nanoscale and hinders the clay layer from stacking; the biocide entrapped/adsorbed within the nanoclay is prevented from interfering with the crosslinking reaction of the organosiloxane oligomers.

The treatments have also shown good consolidating action, as proven by abrasion tests, and chromatic alteration of the substrates can be considered acceptable. Again, the OS_CNaB treatment resulted, albeit slightly, the most performing one.

Finally, preliminary microbiological tests have evidenced that the OS_B and OS_CNaB treatments, containing B at 2%, can effectively inhibit the growth of microorganisms, therefore they can have promising protective effects against microbial colonization when applied on porous substrates as the Neapolitan yellow tuff. Future goals will be the evaluation of both the antimicrobial effectiveness and the activity duration of the treatments by applying them on tuff stones and monitoring during time the microorganisms growing on treated surfaces.

## Funding

This research did not receive any specific grant from funding agencies in the public, commercial, or not-for-profit sectors.

## Declaration of Competing Interest

The authors declare that they have no known competing financial interests or personal relationships that could have appeared to influence the work reported in this paper.

## References

[1] A. Colella, C. Di Benedetto, D. Calcaterra, P. Cappelletti, M. D'Amore, D. Di Martire, S.F. Graziano, L. Papa, A. Langella, The Neapolitan Yellow Tuff: An outstanding example of heterogeneity, Constr. Build. Mater. 136 (2017) 361–373, https://doi.org/10.1016/j.conbuildmat.2017.01.053.
[2] M.D. Jackson, F. Marra, R.L. Hay, C. Cawood, E.M. Winkler, The judicious selection and preservation of tuff and travertine building stone in ancient Rome*, Archaeometry 47 (2005) 485–510, https://doi.org/10.1111/j.1475-4754.2005.00215.x.
[3] D. Calcaterra, P. Cappelletti, A. Langella, A. Colella, M. De Gennaro, The ornamental stones of Caserta province: the Campanian Ignimbrite in the medieval architecture of Casertavecchia, J. Cult. Herit. 5 (2) (2004) 137–148, https://doi.org/10.1016/j.culher.2003.08.003.
[4] A.Z. Miller, A. Dionisio, L. Laiz, M.F. Macedo, C. Saiz-Jimenez, The influence of inherent properties of building limestones on their bioreceptivity to phototrophic microorganisms, Ann. Microbiol. 59 (2009) 705–713, https://doi.org/10.1007/BF03179212.
[5] C.J. McNamara, R. Mitchell, Microbial deterioration of historic stone, Front. Ecol. Environ. 3 (2005) 445–451, https://doi.org/10.2307/3868661.
[6] T. Warscheid, J. Braams, Biodeterioration of stone: a review, Int. Biodeterior. Biodegrad. 46 (2000) 343–368, https://doi.org/10.1016/S0964-8305(00)00109-8.
[7] G.C. Borgia, M. Camaiti, F. Cerri, P. Fantazzini, F. Piacenti, Study of water penetration in rock materials by Nuclear Magnetic Resonance Tomography: hydrophobic treatment effects, J. Cult. Herit. 1 (2000) 127–132, https://doi.org/10.1016/S1296-2074(00)00156-4.
[8] M.J. Heap, J.I. Farquharson, A.R.L. Kushnir, Y. Lavallée, P. Baud, H.A. Gilg, T. Reuschlé, The influence of water on the strength of Neapolitan Yellow Tuff, the most widely used building stone in Naples (Italy), Bull. Volcanol. 80 (2018) 1–15, https://doi.org/10.1007/s00445-018-1225-1.
[9] M. Yavuz Çelik, M. Sert, An assessment of capillary water absorption changes related to the different salt solutions and their concentrations ratios in the Döğer tuff (Afyonkarahisar-Turkey) used as building stone of cultural heritages, J. Build. Eng. 35 (2021), 102102, https://doi.org/10.1016/j.jobe.2020.102102.
[10] J. Tokarský, P. Martinec, K. Mamulová Kutláková, H. Ovčačíková, S. Študentová, J. Ščučka, Photoactive and hydrophobic nano-ZnO/poly(alkyl siloxane) coating for the protection of sandstone, Constr. Build. Mater. 199 (2019) 549–559, https://doi.org/10.1016/j.conbuildmat.2018.12.045.
[11] C.D. Vacchiano, L. Incarnato, P. Scarfato, D. Acierno, Conservation of tuff-stone with polymeric resins, Constr. Build. Mater. 22 (2008) 855–865, https://doi.org/10.1016/j.conbuildmat.2006.12.012.
[12] V. Castelvetro, M. Aglietto, F. Ciardelli, O. Chiantore, M. Lazzari, L. Toniolo, Structure control, coating properties, and durability of fluorinated acrylic-based polymers, J. Coat. Technol. 74 (2002) 57–66, https://doi.org/10.1007/BF02697984.
[13] R. Creasey, J.P. Andrews, S.O. Ekolu, D. Kruger, Long-term 20-year performance of surface coating repairs applied to façades of reinforced concrete buildings, Case Stud. Constr. Mater. 7 (2017) 348–360, https://doi.org/10.1016/j.cscm.2017.11.001.
[14] F. Doğan, H. Dehghanpour, Characterization and hydrophobic surface study of silicon-based TiO2, ZnO and recycled carbon additives on cementitious materials surface, J. Build. Eng. 40 (2021), 102689, https://doi.org/10.1016/j.jobe.2021.102689.
[15] C. Moreau, V. Vergès-Belmin, L. Leroux, G. Orial, G. Fronteau, V. Barbin, Water-repellent and biocide treatments: assessment of the potential combinations, J. Cult. Herit. 9 (4) (2008) 394–400, https://doi.org/10.1016/j.culher.2008.02.002.
[16] G.B. Goffredo, V. Terlizzi, P. Munafò, Multifunctional TiO2-based hybrid coatings on limestone: initial performances and durability over time, J. Build. Eng. 14 (2017) 134–149, https://doi.org/10.1016/j.jobe.2017.10.006.
[17] F. Stazi, A. Nacci, F. Tittarelli, E. Pasqualini, P. Munafò, An experimental study on earth plasters for earthen building protection: the effects of different admixtures and surface treatments, J. Cult. Herit. 17 (2016) 27–41, https://doi.org/10.1016/j.culher.2015.07.009.
[18] H. Okamura, Photodegradation of the antifouling compounds Irgarol 1051 and Diuron released from a commercial antifouling paint, Chemosphere 48 (2002) 43–50, https://doi.org/10.1016/S0045-6535(02)00025-5.
[19] I. Wittmer, R. Scheidegger, C. Stamm, W. Gujer, H. Bader, Modelling biocide leaching from facades, Water Res 45 (2011) 3453–3460, https://doi.org/10.1016/j.watres.2011.04.003.
[20] C. Dresler, M.L. Saladino, C. Demirbag, E. Caponetti, D.F. Chillura Martino, R. Alduina, Development of controlled release systems of biocides for the conservation of cultural heritage, Int. Biodeterior. Biodegrad. 125 (2017) 150–156, https://doi.org/10.1016/j.ibiod.2017.09.007.
[21] P. Manoudis, S. Papadopoulou, I. Karapanagiotis, A. Tsakalof, I. Zuburtikudis, C. Panayiotou, Polymer-silica nanoparticles composite films as protective coatings for stone-based monuments, J. Phys. Conf. Ser. 61 (2007) 1361–1365, https://doi.org/10.1088/1742-6596/61/1/269.
[22] F. Iucolano, A. Colella, B. Liguori, D. Calcaterra, Suitability of silica nanoparticles for tuff consolidation, Constr. Build. Mater. 202 (2019) 73–81, https://doi.org/10.1016/j.conbuildmat.2019.01.002.
[23] L. de Ferri, P.P. Lottici, A. Lorenzi, A. Montenero, E. Salvioli-Mariani, Study of silica nanoparticles – polysiloxane hydrophobic treatments for stone-based monument protection, J. Cult. Herit. 12 (2011) 356–363, https://doi.org/10.1016/j.culher.2011.02.006.
[24] M. Stefanidou, K. Matziaris, G. Karagiannis, Hydrophobization by means of nanotechnology on greek sandstones used as building facades, Geosciences 3 (2013) 30–45, https://doi.org/10.3390/geosciences3010030.
[25] M. Lettieri, M. Masieri, A. Morelli, M. Pipoli, M. Frigione, Oleo/hydrophobic coatings containing nano-particles for the protection of stone materials having different porosity, Coatings 8 (12) (2018) 429, https://doi.org/10.3390/coatings8120429.
[26] J.S. Pozo-Antonio, J. Otero, P. Alonso, X. Mas i Barberà, Nanolime- and nanosilica-based consolidants applied on heated granite and limestone: Effectiveness and durability, Constr. Build. Mater. 201 (2019) 852–870, https://doi.org/10.1016/j.conbuildmat.2018.12.213.
[27] D. Aslanidou, I. Karapanagiotis, Superhydrophobic, superoleophobic and antimicrobial coatings for the protection of silk textiles, Coatings 8 (2018) 101, https://doi.org/10.3390/coatings8030101.
[28] L. D'Arienzo, P. Scarfato, L. Incarnato, New polymeric nanocomposites for improving the protective and consolidating efficiency of tuff stone, J. Cult. Herit. 9 (2008) 253–260, https://doi.org/10.1016/j.culher.2008.03.002.
[29] G. Cappelletti, P. Fermo, M. Camiloni, Smart hybrid coatings for natural stones conservation, Prog. Org. Coat. 78 (2015) 511–516, https://doi.org/10.1016/j.porgcoat.2014.05.029.
[30] A. Chatzigrigoriou, I. Karapanagiotis, I. Poulios, Superhydrophobic coatings based on siloxane resin and calcium hydroxide nanoparticles for marble protection, Coatings 10 (2020) 334, https://doi.org/10.3390/coatings10040334.
[31] l D'orazio, a Grippo, A water dispersed Titanium dioxide/poly(carbonate urethane) nanocomposite for protecting cultural heritage: Preparation and properties, Prog. Org. Coat. 79 (2015) 1–7, https://doi.org/10.1016/j.porgcoat.2014.09.017.
[32] M. Lettieri, A. Calia, A. Licciulli, A.E. Marquardt, R.J. Phaneuf, Nanostructured $TiO_2$ for stone coating: assessing compatibility with basic stone's properties and photocatalytic effectiveness, Bull. Eng. Geol. Environ. 76 (2017) 101–114, https://doi.org/10.1007/s10064-015-0820-z.
[33] P. Scarfato, L. Di Maio, M.L. Fariello, P. Russo, L. Incarnato, Preparation and evaluation of polymer/clay nanocomposite surface treatments for concrete durability enhancement, Cem. Concr. Compos. 34 (4) (2012) 297–305, https://doi.org/10.1016/j.cemconcomp.2011.11.006.

[34] L. Dyshlyuk, O. Babich, S. Ivanova, N. Vasilchenco, A. Prosekov, S. Sukhikh, Suspensions of metal nanoparticles as a basis for protection of internal surfaces of building structures from biodegradation, Case Stud. Constr. Mater. 12 (2020), e00319, https://doi.org/10.1016/j.cscm.2019.e00319.
[35] N. Ditaranto, S. Loperfido, I. Van Der Werf, A. Mangone, N. Cioffi, L. Sabbatini, Synthesis and analytical characterisation of copper-based nanocoatings for bioactive stone artworks treatment, Anal. Bioanal. Chem. 399 (2011) 473–481, https://doi.org/10.1007/s00216-010-4301-8.
[36] I.D. Van Der Werf, N. Ditaranto, R.A. Picca, M.C. Sportelli, L. Sabbatini, Development of a novel conservation treatment of stone monuments with bioactive nanocomposites, Herit. Sci. 3 (29) (2015) 1–9, https://doi.org/10.1186/s40494-015-0060-3.
[37] P. Scarfato, E. Avallone, L. Incarnato, L. Di Maio, Development and evaluation of halloysite nanotube-based carrier for biocide activity in construction materials protection, Appl. Clay Sci. 132–133 (2016) 336–342, https://doi.org/10.1016/j.clay.2016.06.027.
[38] R. Zarzuela, I. Moreno-Garrido, J. Blasco, M.L. Almoraim Gil, M.J. Mosquera, Evaluation of the effectiveness of CuONPs/$SiO_2$-based treatments for building stones against the growth of phototrophic microorganisms, Constr. Build. Mater. 187 (2018) 501–509, https://doi.org/10.1016/j.conbuildmat.2018.07.116.
[39] F. Amor, A. Diouri, I. Ellouzi, F. Ouanji, Development of Zn-Al-Ti mixed oxides-modified cement phases for surface photocatalytic performance, Case Stud. Constr. Mater. 9 (2018), e00209, https://doi.org/10.1016/j.cscm.2018.e00209.
[40] https://www.ctseurope.com/gb/266-silo-112 accessed on February 18, 2022.
[41] S. Mallakpour, M. Dinari, Preparation and characterization of new organoclays using natural amino acids and Cloisite $Na^+$, Appl. Clay Sci. 51 (2011) 353–359, https://doi.org/10.1016/j.clay.2010.12.028.
[42] M.J. Heap, Y. Lavallée, A. Laumann, K.-U. Hess, P.G. Meredith, D.B. Dingwell, How tough is tuff in the event of fire? Geology 40 (4) (2012) 311–314, https://doi.org/10.1130/G32940.1.
[43] UNI EN 15801: Conservation of cultural property - Test methods - Determination of water absorption by capillarity, 2010.
[44] Q. Gao, Z. Ma, J. Xiao, F. Li, Effects of Imposed Damage on the Capillary Water Absorption of Recycled Aggregate Concrete, Adv. Mater. Sci. Eng. 2018 (2018) 1–12, https://doi.org/10.1155/2018/2890931.
[45] M. Cocca, L. D'Arienzo, L. D'Orazio, G. Gentile, E. Martuscelli, In situ polymerisation of urethane-urea copolymers for tuff consolidation, Macromol. Symp. 228 (2005) 245–253, https://doi.org/10.1002/masy.200551022.
[46] Italian Recommendation NORMAL 43/93. Misure colorimetriche di superfici opache, C.N.R - I.C.R., 1993.
[47] P. Cennamo, P. Caputo, A. Giorgio, A. Moretti, N. Pasquino, Biofilms on Tuff Stones at Historical Sites: Identification and Removal by Nonthermal Effects of Radiofrequencies, Microb. Ecol. 66 (2013) 659–668, https://doi.org/10.1007/s00248-013-0247-7.
[48] Y. Xi, R.L. Frost, H. He, Modification of the surfaces of Wyoming montmorillonite by the cationic surfactants alkyl trimethyl, dialkyl dimethyl, and trialkyl methyl ammonium bromides, J. Colloid Interface Sci. 305 (2007) 150–158, https://doi.org/10.1016/j.jcis.2006.09.033.
[49] S. Mallakpour, A. Barati, Application of Modified Cloisite $Na^+$ with L-Phenylalanine for the Preparation of New Poly(vinyl alcohol)/Organoclay Bionanocomposite Films, Polym. Plast. Technol. Eng. 51 (2012) 321–327, https://doi.org/10.1080/03602559.2011.639335.
[50] J.M. Cervantes-UC, J.V. Cauich-Rodriguez, H. Vazquez-Torres, L.F. Garfias-Mesias, D.R. Paul, Thermal degradation of commercially available organoclays studied by TGA-FTIR, Thermochim. Acta 457 (2007) 92–102, https://doi.org/10.1016/j.tca.2007.03.008.
[51] A. Khoshniyat, A. Hashemi, A. Sharif, J. Aalaie, C. Duobis, Effect of surface modification of bentonite nanoclay with polymers on its stability in an electrolyte solution, Polym. Sci. Ser. B 54 (2021) 61–72, https://doi.org/10.1134/S1560090412010034.
[52] L.E. Mardones, M.S. Legnoverde, A.M. Pereyra, E.I. Basaldella, Long-lasting isothiazolinone-based biocide obtained by encapsulation in micron-sized mesoporous matrices, Prog. Org. Coat. 119 (2018) 155–163, https://doi.org/10.1016/j.porgcoat.2018.02.023.
[53] C. Christodoulou, C.I. Goodier, S.A. Austin, J. Webb, G.K. Glass, Long-term performance of surface impregnation of reinforced concrete structures with silane, Constr. Build. Mater. 48 (2013) 708–716, https://doi.org/10.1016/j.conbuildmat.2013.07.038.
[54] A. Rodrigues, B. Sena da Fonseca, A.P. Ferreira Pinto, S. Piçarra, M.F. Montemor, Tailoring alkoxysilanes with poly(ethylene glycol) as potential consolidants for carbonate stones, Constr. Build. Mater. 289 (2021), 123048, https://doi.org/10.1016/j.conbuildmat.2021.123048.
[55] F. Becherini, C. Durante, E. Bourguignon, M. Li Vigni, V. Detalle, A. Bernardi, P. Tomasin, Aesthetic compatibility assessment of consolidants for wall paintings by means of multivariate analysis of colorimetric data, Chem, Cent. J. 12 (2018) 98, https://doi.org/10.1186/s13065-018-0465-7.
[56] C.C. Gaylarde, Influence of environment on microbial colonization of historic stone buildings with emphasis on cyanobacteria, Heritage 3 (4) (2020) 1469–1482, https://doi.org/10.3390/heritage3040081.
[57] M. Farooq, M. Hassan, F. Gull, Mycobial deterioration of stone monuments of Dharmarajika, Taxila, J. Microbiol. Exp. 2 (1) (2015) 29–33, https://doi.org/10.15406/jmen.2015.02.00036.
[58] L. Ruggiero, F. Bartoli, M.R. Fidanza, F. Zurlo, E. Marconi, T. Gasperi, S. Tuti, L. Crociani, E. Di Bartolomeo, G. Caneva, M.A. Ricci, A. Sodo, Encapsulation of environmentally-friendly biocides in silica nanosystems for multifunctional coatings, Appl. Surf. Sci. 514 (2020), 145908, https://doi.org/10.1016/j.apsusc.2020.145908.
[59] J. Eversdijk, S.J.F. Erich, S.P.M. Hermanns, O.C.G. Adanb, M. De Bolle, K. de Meyer, D. Bylemans, M. Bekker, A.T. ten Cate, Development and evaluation of a biocide release system for prolonged antifungal activity in finishing materials, Prog. Org. Coat. 74 (2012) 640–644, https://doi.org/10.1016/j.porgcoat.2011.09.029.